Advances in Materials Research, Vol. 1, No. 1 (2012) 1-12
DOI: http://dx.doi.org/10.12989/amr.2012.1.1.001

One-pot synthesis of gold trisoctahedra with high-index facets

Do Youb Kim[1], Kyeong Woo Choi[1], Sang Hyuk Im**[3], O Ok Park*[1,2]
Xiao-Lan Zhong[4] and Zhi-Yuan Li[4]

[1]*Department of Chemical and Biomolecular Engineering (BK21 graduate program), Korea Advanced Institute of Science and Technology (KAIST), 291 Daehak-ro, Yuseong-gu, Daejeon 305-701, Republic of Korea*
[2]*Department of Energy Systems Engineering, Daegu Gyeongbuk Institute of Science and Technology (DGIST), 50-1, Sang-ri, Hyeonpung-myeon, Dalseong-gun, Daegu 711-873, Republic of Korea*
[3]*KRICT-EPFL Global Research Laboratory, Advanced Materials Division, Korea Research Institute of Chemical Technology (KRICT), 19 Sinseongno, Yuseong-gu, Daejeon 305-600, Republic of Korea*
[4]*Institute of Physics, Chinese Academy of Science, P.O. Box 603, Beijing 100080, People's Republic of China*

(Received September 30 2011, Revised February 23, 2012, Accepted March 16, 2012)

Abstract. There have been many efforts on the generating metal nanocrystals enclosed by high-index facets for the use as highly active catalysts. This paper describes a facile synthesis of Au trisoctahedra with high-index facets. In brief, the Au trisoctahdra were prepared by reduction of $HAuCl_4$ in *N,N*-dimethylformamide (DMF) containing poly (vinyl pyrrolidone) (PVP) and trace amount of $AgNO_3$. The Ag ions in the reaction solution played a critical role in controlling the trisoctahedral shape of the final product by underpotential deposition (UPD) on the Au surfaces. The as-prepared Au trisoctahedra were single crystal and enclosed by high-index {441}, {773} and {331} facets.

Keywords: gold; trisoctahedra; transformation; underpotential deposition; silver

1. Introduction

There have been many interests in shape-controlled synthesis of noble metal nanocrystals, in addition to controlling their size or structure, due to their shape-dependent properties and applications (Burda *et al.* 2005, Xia *et al.* 2005, 2009, Tao *et al.* 2008, Guo *et al.* 2011). Especially, shape-dependent property of metal nanocrystals were clearly shown in the catalytic applications because the nanocrystal shape strongly correlate with not only sharp edges and corners but also their exposed crystallographic facets (Zhou *et al.* 2011, Narayanan *et al.* 2004, Shao *et al.* 2011, Wang *et al.* 2011). Thanks to the efforts from many groups, metal nanocrystals with variety of shapes have been prepared by solution phase synthesis (Burda *et al.* 2005, Xia *et al.* 2005, 2009, Tao *et al.* 2008, Guo *et al.* 2011, Lim *et al.* 2009, Grzelczak *et al.* 2008, Chen *et al.* 2009). Among metal nanocrystals with various shapes, those enclosed by high-index facets have attracted much

*Corresponding author, Professor, E-mail: ookpark@kaist.ac.kr
**Corresponding author, Ph.D., E-mail: imromy@krict.re.kr

attention in recent years because they often exhibit different properties or much enhanced catalytic activities compare to those enclosed by low-index facets (Tian *et al.* 2007, 2008, Ma *et al.* 2008, Yu *et al.* 2011, Jin *et al.* 2011).

In order to precisely control over the shape of metal nanocrystal, foreign metal ions have been often introduced into the reaction. For the gold (Au) nanocrystals, silver (Ag) ions have been widely used for shape control of Au nanocrystals to take advantage of Ag underpotential deposition (UDP) on the Au surfaces, which hinder newly formed Au atoms from being nucleated and grown on the Au surfaces covered with Ag (Kokkinidis 1986, Herrero *et al.* 2001). There has been successful demonstrations that silver Ag ions can induce Au nanocrystals with various shapes (Liu *et al.* 2005, Seo *et al.* 2006, Ming *et al.* 2009, Li *et al.* 2010, Personick *et al.* 2011, Zhang *et al.* 2010). For example, Ming *et al.* (2009) reported the synthesis of tetrahexahedral Au nanocrystals enclosed by {730} facets. Personick *et al.* (2011) reported the syntheses of Au nanocrystals enclosed by low-index facets, such as Au octahedra and rhombic dodecahedra and even those enclosed by high-index facets, such as Au truncated ditetragonal prisms with {310} facets and concave cubes with {720} facets. Although these prior methods could prepare Au nanocrystals enclosed by high-index facets, however, there is still need for the development of a protocol that can generate Au nanocrystals with high-index facets by a facile, one-pot method.

In our previous study, we successfully demonstrated that Au nanocrystals with rhombic dodecahedral shape at the early stage of the reaction could be transformed into those with tetrahexahedral shape through controlled slow growth reaction (Kim *et al.* 2010). It was found that transformation of Au nanocrystals from the rhombic dodecahedral into tetrahexahedral shape was attributed to the relatively fast growth along the <111> and <110> directions than growth along the <100> direction. We speculated that when trace amount of Ag ion was introduced into the reaction, growth rate of Au nanocrystals along these three directions could be controlled by the UDP of Ag on the Au surfaces. Herein, we report the synthesis of Au trisoctahedra with high-index facets via simple reduction of $HAuCl_4$ in *N,N*-dimethylformamide (DMF) in the presence of poly(vinyl pyrrolidone) (PVP) with trace amount of $AgNO_3$. As prepared Au trisoctahedra were single crystalline and enclosed by 24 high-index {441}, {773} and/or {331} facets.

2. Experimetal

2.1 Chemicals

N,N-dimethylformamide (DMF), hydrogen tetrachloroaurate trihydrate ($HAuCl_4 \cdot 3H_2O$), silver nitrate ($AgNO_3$) and poly(vinyl pyrrolidone) (PVP, Mw ≈ 55,000) were all obtained from Sigma-Aldrich and used as received. In the experiment, we used deionized water with a resistivity of 18.2 MΩ/cm, which was prepared using an ultrapure water purification system (Human, Korea).

2.2 Synthesis of Au trisoctahedra

In a typical synthesis, 3.86 mL of DMF was mixed with 0.12 mL of 94.2 mM $HAuCl_4$ and 8 mL of 2.47 M PVP in DMF in a 50 mL glass vial, followed by the introduction of 20 μL of 2 mM $AgNO_3$ aqueous solution. The vial was then capped and then heated to 80°C for ~8 h in an oil bath. It was magnetically stirred during the entire synthesis process. The product was collected by

centrifugation at 10,000 rpm for 5 min, and washed with water and ethanol. The product was finally re-dispersed in ethanol for further characterizations.

2.3 Characterization

The scanning electron microscopy (SEM) images were recorded with a field-emission scanning electron microscope (Sirion, FEI), operated at an accelerating voltage of 20 kV. The energy dispersive X-ray spectroscopy (EDS) analysis was conducted using energy dispersive X-ray spectroscope, which is installed on the SEM (Sirion, FEI). The transmission electron microscopy (TEM) image, selected area electron diffraction (SAED) pattern, and high-resolution TEM (HRTEM) image were recorded with a field-emission transmission electron microscope (JEM-3011, JEOL), operated at an accelerating voltage of 300 kV. The samples were prepared by placing a few drops of the colloidal suspension in ethanol either on silicon substrates for SEM or on copper grids coated with carbon for TEM, SAED, and HRTEM. UV-vis-NIR extinction spectrum of Au trisoctahedra was recorded with a UV-vis-NIR pectrometer (Cary 5000, Varian) with the nanocrystals suspended in ethanol. X-ray diffraction (XRD) pattern was obtained with a X-ray diffractometer (D/MAX-RB, Rigaku) using Cu Kα (0.1542 nm) radiation. The sample for XRD was prepared by repeated dropping and drying of the colloidal suspension in ethanol on silicon substrates. Cyclic voltammetry (CV) measurements were carried out in a three electrode cell using a potentiostat (600C, CH Instrument). The drop-casting films of nanocrystals on indium–tin oxide (ITO) substrates served as working electrodes. Before the CV measurements, the nanocrystals-modified substrates were cleaned by washing with ethanol. Pt wire and Ag/AgCl (in saturated KCl) were used as the counter and reference electrodes, respectively. All cyclic voltammograms were obtained at room temperature. The electrolyte solutions were purged with high-purity N_2 gas before use for about 20 min.

3. Results and discussion

Fig. 1(a) shows typical SEM image of as-prepared nanocrystals, indicating that homogeneous nanocrystals with size ranging from 100 to 180 nm in diameter were successfully synthesized with a yield of over 75%. Trisoctahedron is one of the Archimedean dual or Catalan solids, having 24 triangular faces (Conway *et al.* 2008). The easy way to recognizing the trisoctahedral structure is considering the trisoctahedron as an octahedron surrounded with 8 triangular pyramids at their each triangular surface. There are trisoctahedra with different shapes including their convex and concave structures thus with different exposed surfaces according to the height of triangular pyramids on octahedron's surfaces (Fig. 2). Fig. 1(b) shows SEM images of each individual trisoctahedral nanocrystal in different orientations, which correlate well with schematics of a trisoctahedron in different orientations in the same rows in Fig. 1(c). These trisoctahedral nanocrystals were confirmed as Au trisoctahedra by the EDS analysis (Fig. 3) and the XRD pattern (Fig. 1(d)), which matches well with the face-centered-cubic (*fcc*) structure of Au (JCPDS 4-0784).

We further investigated the crystal structure of Au trisoctahedra by TEM measurement. Fig. 4A shows a low-magnification TEM image of Au trisoctahedra. Fig. 4(b) is a TEM image of single Au trisoctahedron and its corresponding SAED pattern (right top inset) recorded along [011] direction. The bottom right inset is the corresponding schematic of a trisoctahedron oriented along the same

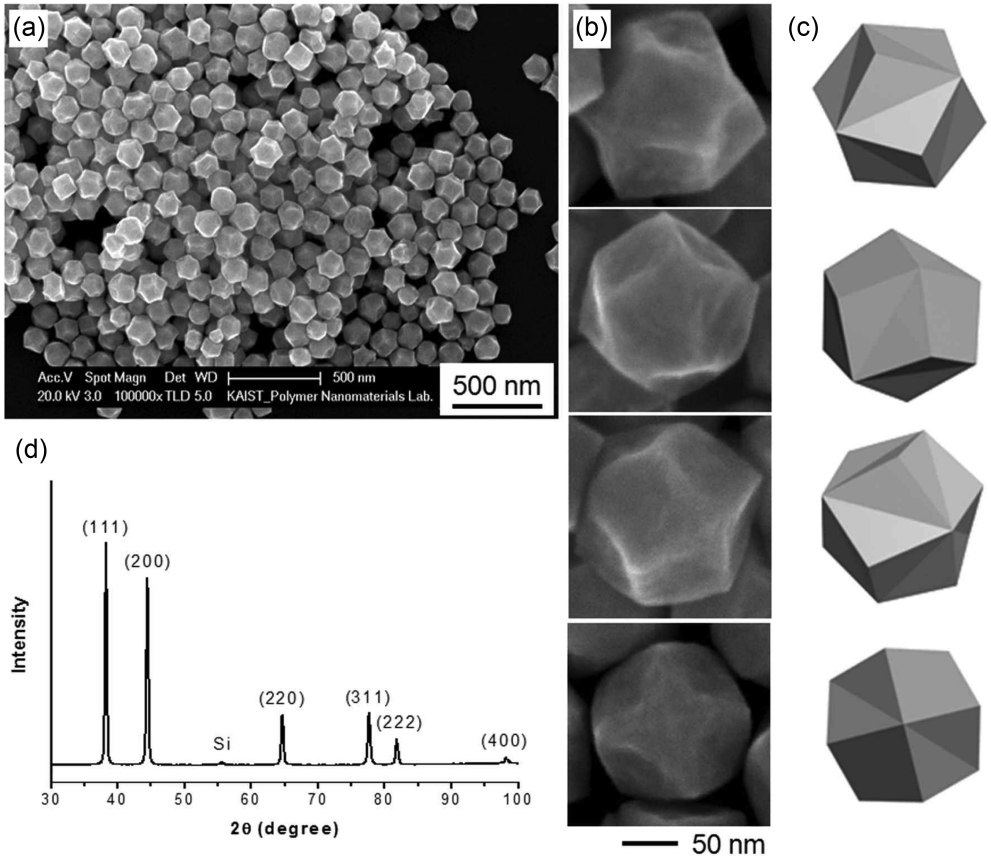

Fig. 1 (a) Low-magnification SEM image of Au trisoctahedra, (b) High-magnification SEM images of Au trisoctahedra in four different orientations, (c) Schematics of a trisoctahedron in four different orientations that correspond to those of the nanoparticles in the same rows in (b), (d) XRD pattern of the Au trisoctahedra on a silicon substrate

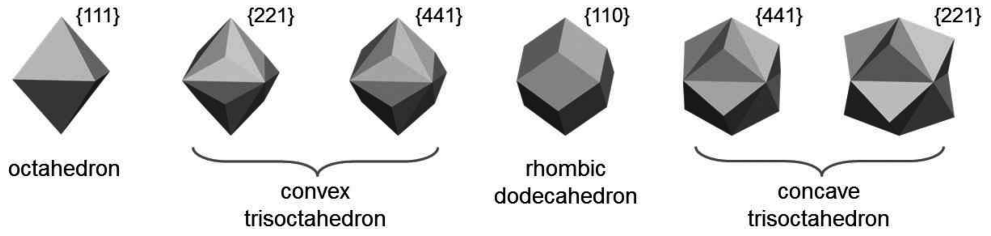

Fig. 2 Schematic diagrams for octahedron, convex and concave trisoctahedra with different facets, and rhombic dodecahedron viewing in the same orientation

direction. The Au trisoctahedron without twin boundaries in the TEM image and spot patterns in SAED indicate that as-prepared Au trisoctahedron is single-crystal (Fig. 4(b)). The HRTEM image (Fig. 4(c)) taken from an individual Au trisoctahedron along the [011] direction shows a continuous fringe pattern with spacing of 0.235, 0.204, and 0.144 nm, which could be indexed to the {111},

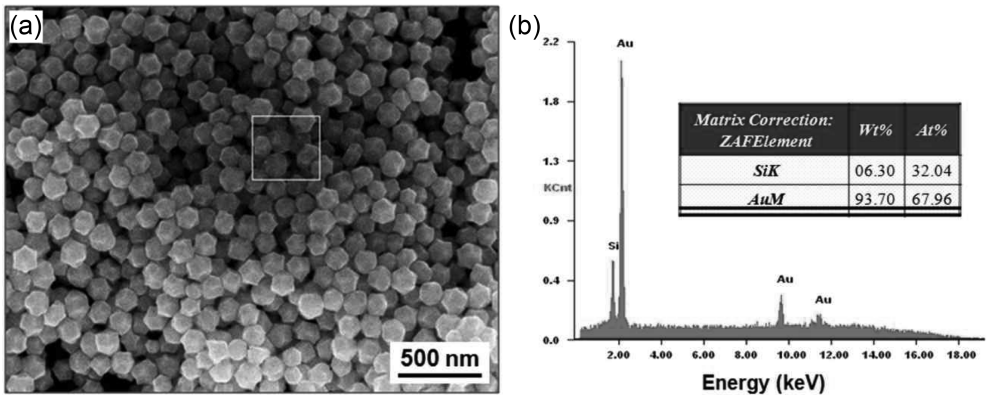

Fig. 3 (a) SEM image of Au trisoctahedra used for EDS analysis, (b) EDS analysis of a drop-cast sample of Au trisoctahedra on a Si wafer

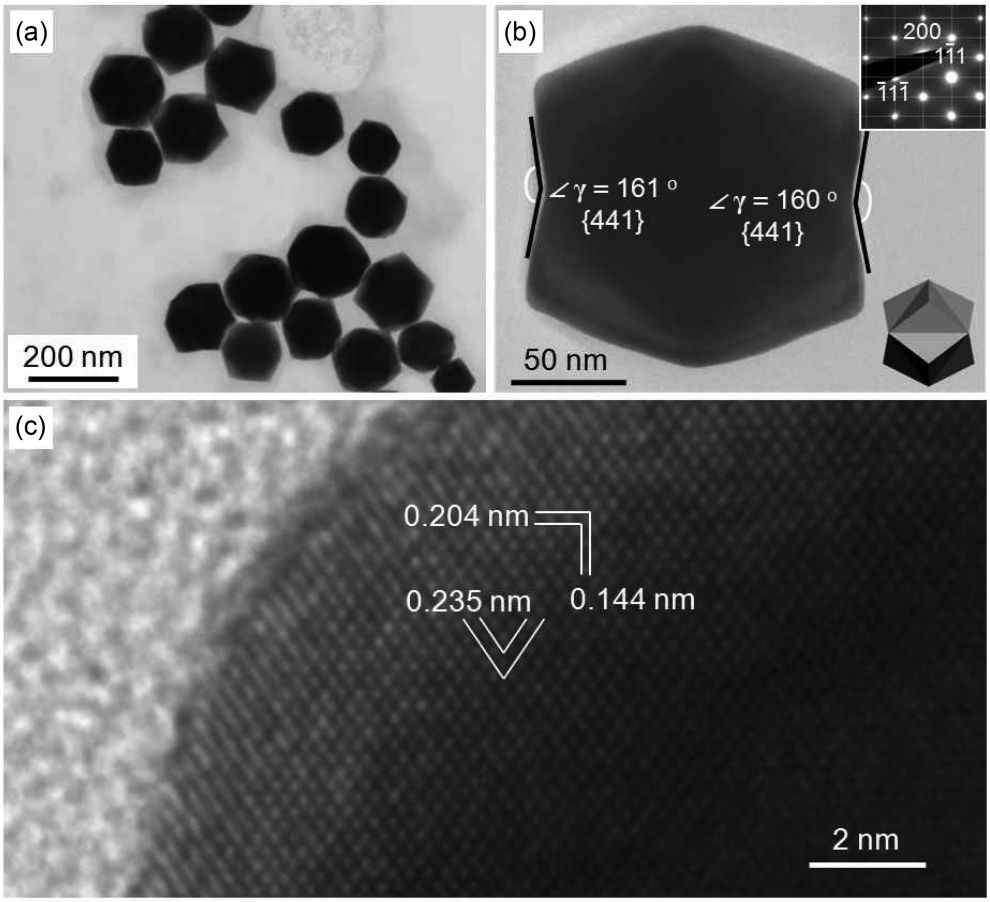

Fig. 4 (a) Low-magnification TEM image of Au trisoctahedra, (b) High-magnification TEM image of a single Au trisoctahedron recorded along the [011] direction. Insets are the corresponding SAED pattern (upper) and a schematic of a trisoctahedron in the same orientation (bottom), (c) HRTEM image taken from the corner region of a Au trisoctahedron

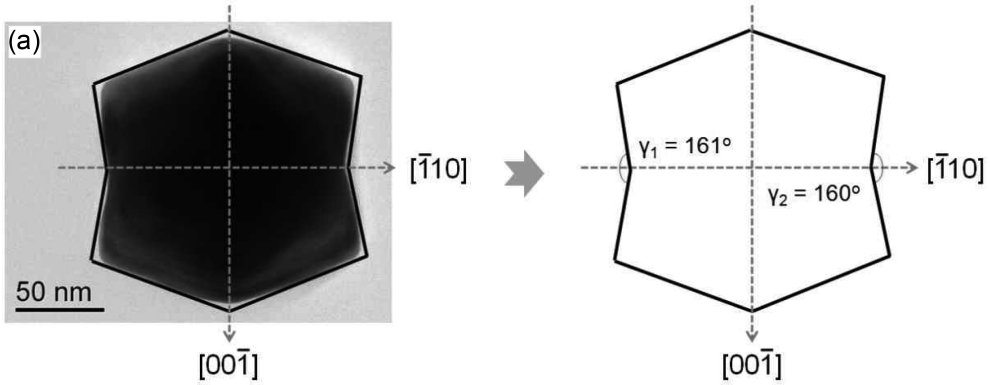

(b)

$$\gamma = 180 - 2\arctan\left(\frac{l}{\sqrt{2}h}\right)$$

angle (γ)	166.6°	163.9°	159.9°	157.2°	153.5°	150.3°	148.4°
{*hhl*}	{661}	{551}	{441}	{772}	{331}	{883}	{552}

Fig. 5 Determination of Miller Indices of exposed facets of Au trisoctahedron, (a) TEM image of single Au trisoctahedron recorded along the <110> direction and its adjacent angles, (b) The equation expressing relation between adjacent angle (γ) and Miller Indices (Tian *et al.* 2008) and table showing the theoretical adjacent angles and different facets of trisoctahedron

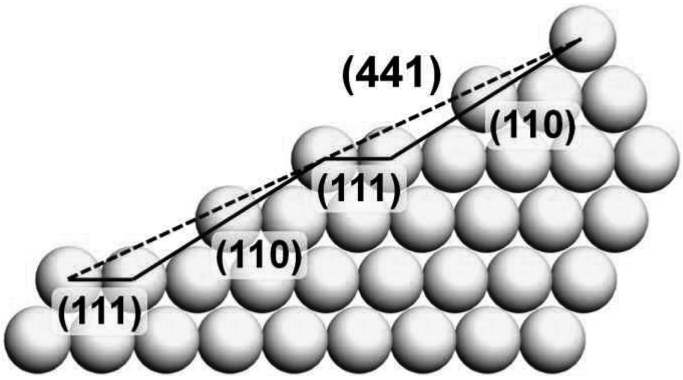

Fig. 6 Atomic model of the Au (441) surface showing the (111) terraces and (110) steps

{200}, and {220} reflections of *fcc* Au, respectively.

The Miller Indices of exposed facets of Au trisoctahedra can be determined by careful measurement of angles between two adjacent facets projected along the [011] zone axis. Although this measurement is indirect method for determining the exposed facets of nanocrystals, it can be used to represent the exposed facets of nanocrystals from the macroscopic view point and the

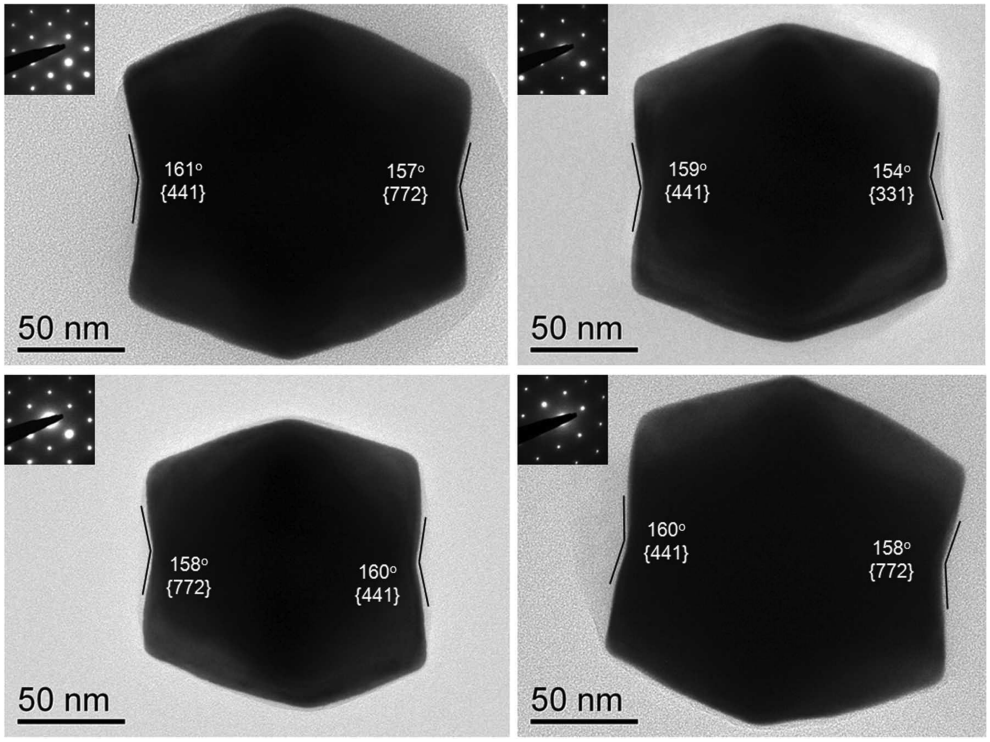

Fig. 7 TEM images of Au trisoctahedra bounded by {441}, {772}, and/or {331} facets and their corresponding SAED patterns (inset)

results obtained by this measurement substantially matched with the results obtained by direct measurement method such as observation the atomic arrangements of nanocrystals by HRTEM analysis (Tian *et al.* 2007, Li *et al.* 2010, Personick *et al.* 2011, Zhang *et al.* 2010). After careful measurements, angles of 161° and 160° were measured as shown in Fig. 4(b). While there were some deviations, these values correspond with theoretical value of angles $\gamma = 159.9°$ between {441} facets (Fig. 5), which clearly indicates that Au trisoctahedron in Fig. 4(b) is bound by {441} high-index facets. As shown in Fig. 6, high-index {441} facet consists of stepped surface with {111} terraces and {110} steps. Although the major facet of the Au trisoctahedra is {441}, we could also observe that there were Au trisoctahedra with other high-index facets such as {772} and {331}, which are the vicinal facets with {441} (Fig. 7).

The surface structure of the Au trisoctahedra was also characterized by cyclic voltammetry (CV). The electrochemical behavior of the Au trisoctahedra on an indium-tin oxide electrode was different from that of the Au octahedra enclosed by low-index {111} facets (Fig. 8). This result suggests that the as-prepared Au nanocrystals are not enclosed by low-index facets, consistent with the SEM and TEM observations.

Although the formation mechanism of Au trisoctahedra is still, for the present, unclear, we believe that the presence of Ag ions in the reaction solution give rise to the trisoctahedral morphology. In order to verify the formation mechanism of Au trisoctahedra, we conducted a control experiment to confirm the effect of water on the shape of resultant Au nanocrystals. It has been known that water

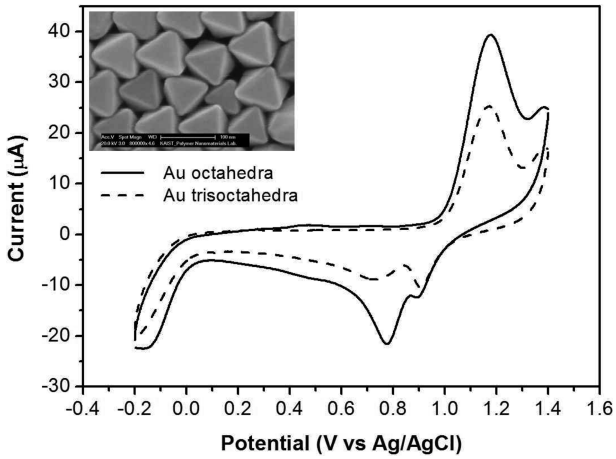

Fig. 8 CV of Au octahedra and trisoctahedra on an ITO electrode with a scan rate of 20 mVs^{-1} in 0.1 M $HClO_4$. Inset is corresponding SEM image of Au octahedra prepared according to a previous procedure (Kim *et al.* 2010)

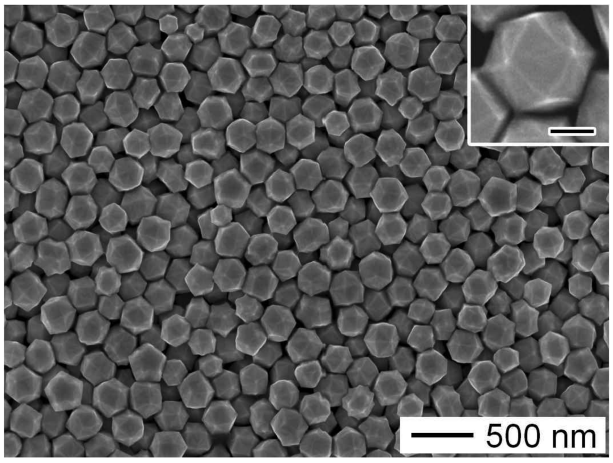

Fig. 9 SEM image of Au nanocrystals prepared under the same condition with those for Fig. 1 except that 20 μL of $AgNO_3$ (2 mM) aqueous solution was replaced by the same volume of deionized water. Inset is the corresponding, high-magnification SEM image. The scale bar in inset represents 100 nm

plays a critical role in shape of resultant Au nanocrystals under the experimental system, which uses DMF as both a reducing agent and solvent (Kim *et al.* 2010, 2011). When deionized water instead of $AgNO_3$ aqueous solution with the same amount (20 μL) was added into the reaction solution, Au tetrahexahedra instead of trisoctahedra were obtained (Fig. 9). This result indicates that Ag ions rather than water in the reaction solution played a key role on the formation of the Au trisoctahedra. It seemed that relatively small amount of water (20 μL, 1/600 of total volume) was insufficient to have influence on the shape of Au nanocrystals. Fig. 10 shows a schematic diagram for transformation of a rhombic dodecahedron into a trisoctahedron viewing from the same direction, [100] and [110] directions, respectively. As shown, it is easily recognized that a rhombic

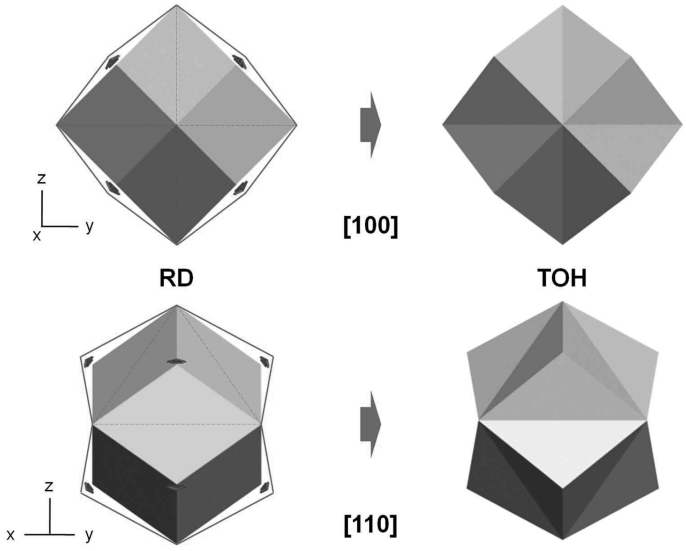

Fig. 10 Schematic illustration showing the transformation of the rhombic dodecahedron into the trisoctahedron viewing from [100] (upper row) and [110] (bottom row) directions, respectively. Models in the same row indicate a rhombic dodecahedron (left) and a trisoctahedron (right), respectively. The red arrows indicate the growing along the <111> direction

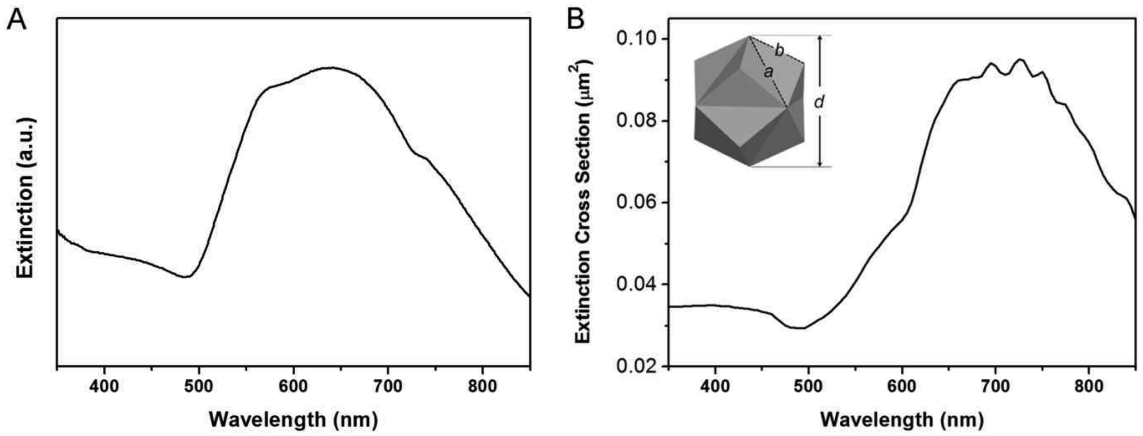

Fig. 11 (a) Experimetally measured and (b) calculated UV-vis-NIR extinction spectra of the Au trisoctahedra

dodecahedron could be transformed into a trisoctahedron with the relatively fast growing along the <111> direction than the other directions. Note that when no Ag ion was involved in the reaction solution, Au rhombic dodecahedra were transformed into Au tetrahexahedra through the faster growth along the <111> and <110> directions than growth along the <100> direction (Kim *et al.* 2010). In the present experiment, Ag ions in the reaction solution seemed to generate monolayer over Au{110} facets and protect the facets from further growth through UDP, leading Au nanocrystals grew along the <111> direction relatively faster than along the <110> and <100> directions. This result is well consistent with the previous report that Ag ions strongly affect the

growth rate of Au nanocrystals through UDP of metallic Ag on the different crystallographic facets of Au and the UDP shifts of Ag on Au surfaces are in the order of {110} > {100} > {111} (Liu *et al*. 2005, Carbó-Argibay *et al.* 2010).

The Au nanocrystals with well-defined morphologies exhibit distinct optical properties, which is associated with the surface plasmons (Burda *et al*. 2005). We also examined the optical property of the Au trisoctahedra using UV-vis-NIR spectrometer and compared with that of theoretically calculated. Fig. 11(a) and (b) show the experimentally measured and calculated UV-vis-NIR extinction spectra of the Au trisoctahedra, respectively. The calculation for the Au trisoctahedra was based on discrete dipole approximation (DDA) method. The inset in the Fig. 10(b) is a model of a trisoctahedron for this calculation, where *a* and *b* represent edge length of octahedron and triangular pyramids surrounded on the faces of the octahedron, respectively. We assumed *a* and *b* as 100 nm and 75 nm, respectively, and thus the diameter (*d*) of the Au trisoctahedron should be ca. 141 nm. Both of the spectra show dipole and higher-order multipole resonances (Fig. 11(a) and (b)). Some differences in peak positions and broadness between the experimentally measured spectrum and the calculated one are possibly due to the size distribution of the Au trisoctahedra and the degree of truncation in their edge and vertices.

4. Conclusions

In conclusion, Au trisoctahedra bound to 24 high-index such as {441}, {773} and/or {331} facets were successfully synthesized by a facile colloidal chemistry by reduction of $HAuCl_4$ in DMF in the presence of PVP and trace amount of $AgNO_3$ (molar ratio of Ag/Au ≈ 1/280). UDP of Ag on the Au surface was essential to the formation of the Au trisoctaehdra in addition to the slow reduction rate. The as-prepared Au trisoctahedra exhibited distinct optical properties. This approach may provide a simple route to the shape-controlled synthesis of metal nanocrystals with high surface energies.

Acknowledgements

This work was supported by the WCU (World Class University) program through the National Research Foundation of Korea (NRF) funded by the Ministry of Education, Science and Technology (MEST) (R32-2008-000-10142-0). This research was also partially supported by the Public welfare&Safety research program through the NRF funded by the MEST (2011-0028468).

References

Burda, C., Chen, X., Narayanan, R. and El-Sayed, M.A. (2005), "Chemistry and properties of nanocrystals of different shapes", *Chem. Rev.*, **105**(4), 1025-1102.

Carbó-Argibay, E., Rodríguez-González, B., Gómez-Graña, S., Guerrero-Martínez, A., Pastoriza-Santos, I., Pérez-Juste, J. and Liz-Marzán, L.M. (2010), "The crystalline structure of gold nanorods revisited: evidence for higher-index lateral facets", *Angew. Chem. Int. Edit.*, **49**(49), 9397-9400.

Chen, J., Lim, B., Lee, E.P. and Xia, Y. (2009), "Shape-controlled synthesis of platinum nanocrystals for catalytic and electrocatalytic applications", *Nano Today*, **4**(1), 81-95.

Conway, J.H., Burgiel, H. and Goodman-Strauss, C. (2008), *The symmetries of things*, Ed. A.K. Peters, Wellesley, MA.
Grzelczak, M., Pérez-Juste, J., Mulvaney, P. and Liz-Marzán, L.M. (2008), "Shape control in gold nanoparticle synthesis", *Chem. Soc. Rev.*, **37**(9), 1783-1791.
Guo, S. and Wang, E. (2011), "Noble metal nanomaterials: Controllable synthesis and application in fuel cells and analytical sensors", *Nano Today*, **6**(3), 240-264.
Herrero, E., Buller, L.J. and Abruña, H. (2001), "Underpotential deposition at single crystal surfaces of Au, Pt, Ag and other materials", *Chem. Rev.*, **101**(7), 1897-1930.
Jin, M., Zhang, H., Xie, Z. and Xia, Y. (2011), "Palladium concave nanocubes with high-index facets and their enhanced catalytic properties", *Angew. Chem. Int. Edit.*, **50**(34), 7850-7854.
Kim, D.Y., Im, S.H. and Park, O.O. (2010), "Synthesis of tetrahexahedral gold nanocrystals with high-index facets", *Cryst. Growth Des.*, **10**(8), 3321-3323.
Kim, D.Y., Im, S.H., Park, O.O. and Lim, Y.T. (2010), "Evolution of gold nanoparticles through catalan, archimedean, and platonic solids", *Cryst. Eng. Comm.,* **12**(1), 116-121.
Kim, D.Y., Li, W., Ma, Y., Yu, T., Li, Z.Y., Park, O.O. and Xia, Y. (2011), "Seed-mediated synthesis of gold octahedra in high purity and with well-controlled sizes and optical properties", *Chem. Eur. J.*, **17**(17), 4759-4764.
Kokkinidis, G. (1986), "Underpotential deposition and electrocatalysis", *J. Electroanal. Chem.*, **201**(2), 217-236.
Li, J., Wang, L., Liu, L., Guo, L., Han, X. and Zhang, Z. (2010), "Synthesis of tetrahexahedralAunanocrystals with exposed high-index surfaces", *Chem. Commun.*, **46**(28), 5109-5111.
Lim, B., Jiang, M., Tao, J., Camargo, P.H.C., Zhu, Y. and Xia, Y. (2009), "Shape-controlled synthesis of Pd nanocrystals in aqueous solutions", *Adv. Func. Mater.*, **19**(2), 189-200.
Liu, M. and Guyot-Sionnest, P. (2005), "Mechanism of silver(I)-assisted growth of gold nanorods and bipyramids", *J. Phys. Chem. B*, **109**(47), 22192-22200.
Ma, Y., Kuang, Q., Jiang , Z., Xie, Z., Huang, R. and Zheng, L. (2008), "Synthesis of trisoctahedral gold nanocrystals with exposed high-index facets by a facile chemical method", *Angew. Chem. Int. Edit.*, **47**(46), 8901-8904.
Ming, T., Feng, W., Tang, Q., Wang, F., Sun, L., Wang, J. and Yan, C. (2009), "Growth of tetrahexahedral gold nanocrystals with high-index facets", *J. Am. Chem. Soc.*, **131**(45), 16350-16351.
Narayanan, R. and El-Sayed, M.A. (2004), "Shape-dependent catalytic activity of platinum nanoparticles in colloidal solution", *Nano Lett.*, **4**(7), 1343-1348.
Personick, M.L., Langille, M.R., Zhang, J. and Mirkin, C.A. (2011), "Shape control of gold nanoparticles by silver underpotential deposition", *Nano Lett.*, **11**(8), 3394-3398.
Seo, D., Park, J.C. and Song, H. (2006), "Polyhedral gold nanocrystals with oh symmetry: from octahedra to cubes", *J. Am. Chem. Soc.*, **128**(46), 14863-14870.
Shao, M., Yu, T., Odell, J.H., Jin, M. and Xia, Y. (2011), "Structural dependence of oxygen reduction reaction on palladium nanocrystals", *Chem. Commun.*, **47**(23), 6566-6568.
Tao, A.R., Habas, S. and Yang, P. (2008), "Shape control of colloidal metal nanocrystals", *Small*, **4**(3), 310-325.
Tian, N., Xhou, Z.Y., Sun, S.G., Ding, Y. and Wang, Z.L. (2007), "Synthesis of tetrahexahedral platinum nanocrystals with high-index facets and high electro-oxidation activity", *Science*, **316**(5825), 732-735.
Tian, N., Zhou, Z.Y. and Sun, S.G. (2008), "Platinum metal catalysts of high-index surfaces: From single-crystal planes to electrochemically shape-controlled nanoparticles", *J. Phys. Chem. C*, **112**(50), 19801-19817.
Wang, J., Gong, J., Xiong, Y., Yang, J., Gao, Y., Liu, Y., Lu, X. and Tang, Z. (2011), "Shape-dependent electrocatalytic activity of monodispersed gold nanocrystals toward glucose oxidation", *Chem. Commun.*, **47**(24), 6894-6896.
Xia, Y. and Halas, N.J. (2005), "Shape-controlled synthesis and surface plasmonic properties of metallic nanostructures", *Mater. Res. Soc. Bull.*, **30**(5), 338-348.
Xia, Y., Xiong, Y., Lim, B. and Skrabalak, S.E. (2009), "Shape-controlled synthesis of metal nanocrystals: simple chemistry meets complex physics?", *Angew. Chem. Int. Edit.*, **48**(1), 60-103.
Yu, T., Kim, D.Y., Zhang, H. and Xia, Y. (2011), "Platinum concave nanocubes with high-index facets and their enhanced activity for oxygen reduction reaction", *Angew. Chem. Int. Edit.*, **50**(12), 2773-2777.
Yu, Y., Zhang, Q., Xie, J., Lu, X. and Lee, J.Y. (2011), "Synthesis of shield-like singly twinned high-index Au

nanoparticles", *Nanoscale*, **3**(4), 1497-1500.
Zhang, J., Langille, M.R., Personick, M.L., Zhang, K., Li, S. and Mirkin, C.A. (2010), "Concave cubic gold nanocrystals with high-index facets", *J. Am. Chem. Soc.*, **132**(40), 14012-14014.
Zhou, Z.Y., Tian, N., Li, J.T., Broadwell, I. and Sun, S.G. (2011), "Nanomaterials of high surface energy with exceptional properties in catalysis and energy storage", *Chem. Soc. Rev.*, **40**(7), 4167-4185.